A Circularly Permuted Myoglobin Possesses a Folded Structure and Ligand Binding Similar to Those of the Wild-Type Protein but with a Reduced Thermodynamic Stability†

Anna L. Fishburn,‡,§ Jennifer R. Keeffe,‡,|| Alexei V. Lissounov,‡ David H. Peyton,⊥ and Spencer J. Anthony-Cahill*,‡

Department of Chemistry, Western Washington University, Bellingham, Washington 98225-9150, and Department of Chemistry, Portland State University, Portland, Oregon 97207-0751

Received July 3, 2002; Revised Manuscript Received August 27, 2002

ABSTRACT: A circular permutein of sperm whale myoglobin in which the G helix is C-terminal, the H helix is N-terminal, and 16 amino acids link the H helix to the A helix has been expressed in *Escherichia coli*. The permutein sequence begins with Gly121 (using the numbering scheme for the wild-type protein) and terminates with Pro120. The ligand binding function of the permutein was assayed using stopped-flow methods and shown to be essentially identical to that of the wild-type protein. In addition, one- and two-dimensional NMR studies of the cyanomet isoform of the permutein show a nativelike structure with a heme binding pocket very similar to that of the wild-type myoglobin. Although the structure and function of the permutein resemble those of the wild-type myoglobin, the permutein is less stable to chemical denaturation by 5.2 kcal/mol.

An understanding of the principles that determine protein folding and stability is fundamentally important to the rational design of proteins with novel functional properties. Much protein design research has been directed toward achieving greater stability in proteins (*1*−*7*); however, in many cases, the desired protein activity is not correlated with the greatest thermal or chemical stability (*8*), so stability and activity must be balanced when designing a novel protein. An understanding of the effects of topological mutations (e.g., the rearrangement of the sequence of secondary structural elements in a protein) on protein structure, stability, and activity will enhance the work of protein researchers who must strike this balance when designing the therapeutics (*9*−*11*), diagnostics, and process catalysts of the future. In addition, protein folding is an important concern, since designed proteins must fold to the desired active structures. A better understanding of the factors that influence protein folding could not only improve designs of novel proteins but also aid the development of accurate methods for the prediction of functional structures from protein primary sequence.

A detailed understanding of the sequence of events in a protein folding pathway will contribute to greater success in the design of proteins that will fold efficiently. Isotope exchange experiments (*12*, *13*) and perturbation analysis (*14*, *15*) have been used to elucidate the structures of folding intermediates and transition state structures. Recently, "circular permutation" has been used to create proteins with topological mutations, and thereby to identify the so-called "folding elements" within a protein (*16*−*18*). A folding element is defined as that part of a protein sequence that must remain intact for the protein to fold properly. A "permutein" contains the same sequence elements of the parent protein, but these elements are arranged in an altered order (Figure 1). In a "circular permutein", the connections between sequence elements are altered in two places compared to the parent protein. (1) There is a new peptide linker covalently connecting the wild-type termini, and (2) there is an "amide cleavage" to create the new permuted termini. To define systematically the folding elements of a protein, one can generate all possible permuteins in a directed fashion (*18*), or use random cloning methods to generate a library of all possible permuted sequences (*17*, *19*, *20*).

We are probing the relationship between protein topology and folding using circular permuteins of sperm whale myoglobin (swMb).[1] Four considerations make swMb an excellent model system for this work. First, swMb is a small (17 kDa) protein that has been expressed at high levels in bacterial systems from a synthetic gene composed of optimal *Escherichia coli* codons (*21*). Second, extensive structural and biophysical characterization of holo- and apomyoglobins has been reported (see refs *22*−*33*). Third, the results obtained with myoglobin permuteins can be used to design topological changes in structurally related globin proteins. The use of swMb as a good predictive model system for the engineering of recombinant human hemoglobin has been

† Supported by grants from Research Corp. (CC4632) and ACS-PRF (35195-B4) and summer undergraduate student research grants from the Jean Dreyfus-Boissevain Scholarship (to A.L.F.) and from Zymogenetics, Inc. (to J.R.K.).

* To whom correspondence should be addressed. E-mail: sacahill@chem.wwu.edu. Telephone: (360) 650-3152. Fax: (360) 650-2826.

‡ Western Washington University.

§ Current address: Fred Hutchinson Cancer Research Center, 1100 Fairview Ave. N., Seattle, WA 98109.

|| Current address: Department of Biochemistry, University of Washington, Box 357350, Seattle, WA 98195-7742.

⊥ Portland State University.

10.1021/bi026404g CCC: $22.00
Published on Web 10/09/2002

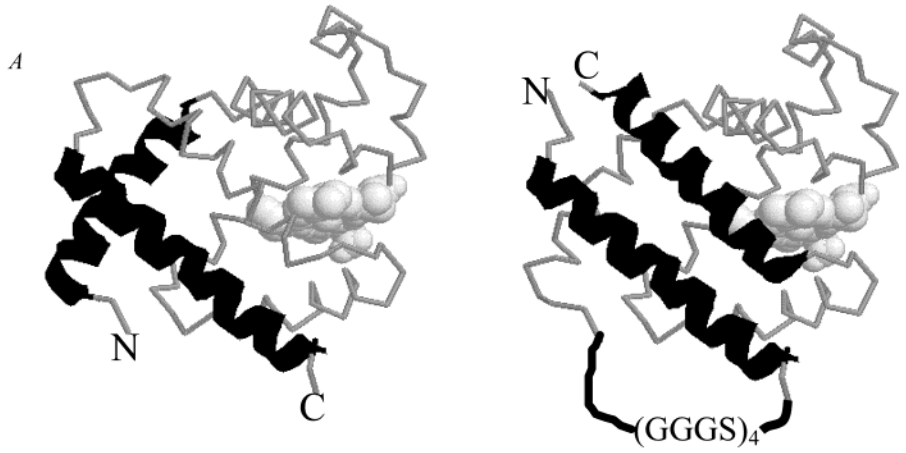

B GDFGADAQGAMNKALELFRKDIAAKYKELGYQG*SGGGSGGGSG*
*GGSGGG*VLSEGEWQLVLHVWAKVEADVAGHGQDILIRLFKSHPE
TLEKFDRFKHLKTEAEMKASEDLKKHGVTVLTALGAILKKKGHH
EAELKPLAQSHATKHKIPIKYLEFISEAIIHVLHSRHP

FIGURE 1: (A) Backbone rendering of wild-type swMb (left) and a schematic drawing of HGL16 permutein (right). The N- and C-terminal helices are shown as dark ribbons. Note that the order of the amino acids in the permutein linker is reversed to reflect the N → C terminal orientation of the linker, as shown in the figure. (B) Primary sequence of HGL16. The 16 amino acids in the linker are shown in italics.

established in the case of heme pocket mutations (*34*−*36*), and the permutation of human alpha globins has been reported recently (*37*). Fourth, the folding pathway of apomyoglobin has been extensively studied (see refs *13*, *28*, *31*, *32*, and *38*−*40* and references therein). The alteration of topology has been shown to affect protein folding kinetics (*41*, *42*); thus, permuteins of swMb would be useful for improving our understanding of the folding mechanism of this protein and testing predictions for early folding events (*43*).

EXPERIMENTAL PROCEDURES

General. The following commercially available strains of *E. coli* were used for cloning and expression experiments: DH5α, XL1-blue, and BL21(DE3). Enzymes were purchased from New England Biolabs. The gene for sperm whale myoglobin in pUC19, originally described by Springer and Sligar (*21*), was provided by J. Olson. Synthetic oligonucleotides were ordered from Sigma-Genosys (The Woodlands, TX). Dideoxy sequencing was performed at Thetagen Inc. (Bothell, WA) or Davis Sequencing LLC (Davis, CA). Protein sequence analysis was performed by the laboratory of R. Paxton (Immunex Corp., Seattle, WA), and protein mass spectral analysis was performed by the laboratory of R. Johnson (Immunex Corp.). Protein concentrations were calculated at pH 7.0 using the following extinction coefficients: $\epsilon_{418} = 128\ mM^{-1}\ cm^{-1}$ and $\epsilon_{280} = 36.6\ mM^{-1}\ cm^{-1}$ for oxymyoglobins and $\epsilon_{423} = 109.7\ mM^{-1}\ cm^{-1}$ for cyanometmyoglobins (*44*).

Scheme 1: Construction of the swMb Tandem Gene Template[a]

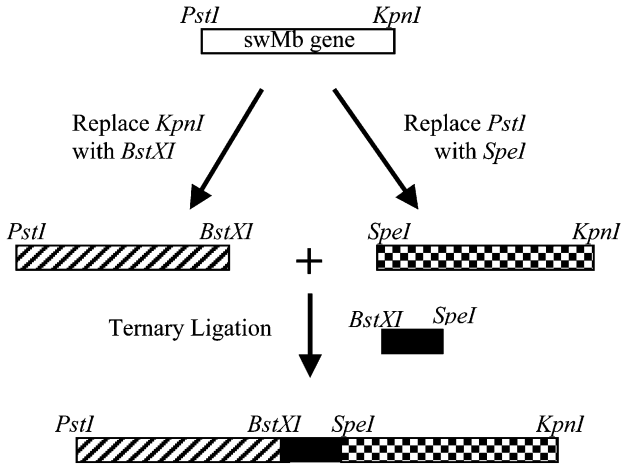

[a] Two copies of the swMb gene were amplified from the wild-type gene and then ligated in-frame with the linker sequence (solid rectangle) to yield the tandem gene.

Construction of the Tandem swMb Gene Template. The construction of the tandem swMb gene is illustrated in Scheme 1. The swMb gene described by Springer and Sligar was amplified by primer extension using two sets of primers. The first set (5′-CCAAGCTTGCATGCCTGCAG-3′ and 5′-GGTACCTCCATCCATAACCCTGGTAACCC-3′) yielded a dsDNA fragment that encodes a swMb gene sequence with a 5′ *Pst*I site and a 3′ *Bst*XI site. The second set (5′-ATGGCAACTAGTTCTGCATGTTTGGG-3′ and 5′-GAGCTCGGTACCCATTAACCC-3′) yielded a dsDNA fragment that encodes a swMb gene sequence with a 5′ *Spe*I site and a 3′ *Kpn*I site. These DNA frag-

[1] Abbreviations: swMb, recombinant sperm whale myoglobin; HGL16, circularly permuted myoglobin that begins with Gly121 and has 16 amino acids connecting the original N- and C-termini; CD, circular dichroism; NMR, nuclear magnetic resonance; SUPERWEFT, super-water elimination Fourier transform spectroscopy; NOESY, nuclear Overhauser effect spectroscopy; COSY, correlation spectroscopy; TPPI, time-proportional phase incrementation; K_{CO}, equilibrium association constant for CO binding; K_{O_2}, equilibrium association constant for O_2 binding; $\Delta G°_{H_2O}$, free energy of unfolding at zero denaturant concentration; m_g, dependence of the free energy of unfolding on denaturant concentration; C_m, concentration of denaturant at the midpoint of the unfolding transition; IPTG, isopropyl thiogalactoside; SDS−PAGE, sodium dodecyl sulfate−polyacrylamide gel electrophoresis; IMAC, immobilized metal affinity chromatography; HPSEC, high-pressure size exclusion chromatography.

ments were restricted with *Bst*XI and *Spe*I, respectively. A synthetic dsDNA cassette encoding the sequence Gly(SerGlyGlyGly)$_4$ValLeuSerGluGlyGluTrpGlnLeu was constructed from the following complementary oligonucleotides: 5′-CTGGTGGTGGTTCTGGTGGTGGTTCTGGTGGTGGTTCTGGTGGTGGTGTTTTGTCTGAGGGTGAGTGGCAA-3′ and 5′-CTAGTTGCCACTCACCCTCAGACAAAACACCACCACCAGAACCACCACCAGAACCACCACCAGAACCACCACCAGAACC-3′. The cassette contains a 5′ *Bst*XI site and a 3′ *Spe*I site, and encodes the 16 amino acids in the linker as well as the C-terminal Gly from the upstream copy of the swMb gene and the 10 N-terminal amino acids from the downstream copy of the swMb gene. The linker and the two restricted gene fragments were ligated together. The resulting ligation mixture was amplified using the primers 5′-CCAAGCTTGCATGCCTGCAG-3′ and 5′-GAGCTCGGTACCCATTAACCC-3′ to yield the desired tandem gene fragment. The tandem gene fragment was restricted with *Pst*I and *Kpn*I and ligated into pUC19. The sequence of the tandem construct was verified by dideoxy sequencing.

Construction of the HGL16 Gene. The gene encoding the HGL16 permutein of swMb was amplified from the swMb tandem gene template using the following primers: 5′-CATGCCATGGGTGACTTCGGTGCTACGCT-3′ and 5′-ATAACTGCAGTCATCATGGATGTCTAGAATGCAGAACAT-3′. The resulting dsDNA fragment was gel-purified, restricted with *Nco*I and *Pst*I, and ligated into pTrc99a (Amersham Pharmacia Biotech). The ligated plasmid was transformed into *E. coli* strain DH5α. Transformed cells were grown on LB/ampicillin (50 μg/mL) agar plates overnight, and candidate clones were screened by restriction analysis to confirm the presence of the permutein gene. The HGL16 gene sequence was confirmed by dideoxy sequencing.

Protein Expression and Purification. All recombinant proteins were expressed in 1 L shake flask cultures at 37 °C. The *E. coli* strains containing wild-type and permuted swMb genes were grown in LB with 50 μg/mL ampicillin until mid-log phase (OD_{600} = 0.4−0.6) and then induced with 0.1 mM IPTG. Wild-type swMb cultures were incubated for 16 h postinduction and then harvested by centrifugation. Cultures of HGL16 were incubated for 4−5 h postinduction and then harvested by centrifugation. The harvested cells (3−5 mL) were resuspended in approximately 25 mL of lysis buffer [50 mM Tris-HCl and 17 mM NaCl (pH 8.5)] and then lysed by sonication (90 s). The crude cell lysate was then centrifuged at 21000*g* for 20 min, and the supernatant was retained. The pH of the supernatant was adjusted to 8.0−8.5, and zinc acetate was added to a final concentration of 2 mM. The lysate was centrifuged at 40000*g* for 20 min and then filtered through a 0.45 μm filter. The filtered lysate was then loaded onto a column packed with 3 mL of IMAC resin (Amersham Pharmacia Biotech Chelating Sepharose Fast Flow) charged with zinc acetate. The column was washed with buffer as follows: 24 mL of 20 mM Tris-HCl and 0.5 M NaCl (pH 8.5), then 24 mL of 250 mM Tris-HCl (pH 8.5), and finally 24 mL of 20 mM Tris-HCl (pH 8.5). The protein was then eluted from the column with 20 mM Tris-HCl and 15 mM EDTA (pH 8.5). The eluant was collected in 1 mL fractions, and those fractions containing significant absorbance at 418 nm were pooled. IMAC-purified proteins were concentrated (Amicon Centricon YM-10 concentrators) until the total volume was approximately 300−700 μL, and 100−300 μL was then injected onto an HPSEC column (Amersham Pharmacia Biotech Superdex 75 HR 10/30) attached to an HPLC system (Varian ProStar) and equilibrated with 20 mM Tris-HCl and 150 mM NaCl (pH 8.0). The absorbance at 280 nm was monitored, and fractions corresponding to peaks at this absorbance as well as peaks at 418 nm were collected. Pooled fractions were concentrated as described above to a final myoglobin concentration of approximately 0.5 mM. All proteins were determined to be greater than 95% homogeneous by SDS−PAGE. Protein masses were confirmed by mass spectral analysis (MALDI-TOF) of the purified proteins and their tryptic fragments.

Determination of Ligand Binding Kinetic Constants. Ligand binding kinetics were determined in the laboratory of J. Olson using a Gibson-Dionex stopped-flow apparatus equipped with an OLIS model 3820 data collection system as described by Rohlfs et al. (*35*). Protein solutions were made up in degassed 0.1 M potassium phosphate and 0.3 mM EDTA (pH 7.0) to a concentration of 5 μM. For association rate experiments, deoxy-Mb was mixed with CO- or O_2-saturated buffers under pseudo-first-order conditions at 20 °C. Dissociation reactions were carried out by mixing the ligand-bound complex with a solution of a displacing ligand. For O_2 off-rate determinations, the displacing ligand was CO, and for the CO off-rate determinations, the displacing ligand was NO. Association rates were also measured by laser flash photolysis using stoppered cuvettes with known concentrations of the ligand. Kinetic constants were calculated from data collected at three to five different ligand concentrations.

Chemical Denaturation Studies. Chemical denaturation studies were carried out at 25 °C using freshly prepared urea (USB, ultrapure grade) in 10 mM potassium phosphate and 100 mM KCl (pH 7.5). The concentration of urea was determined by the refractive index (*45*). A concentrated stock solution of the purified holoprotein was oxidized to the aquomet isoform with 1.1 heme equivalents of potassium ferricyanide immediately prior to dilution of the stock with buffer containing urea. UV−vis measurements at 409 nm were taken using a Hewlett-Packard 8453 UV−vis spectrometer with masked 1 cm path length cuvettes. CD was measured at 222 nm using an OLIS DSM-10 CD spectrometer and circular 1 mm path length cuvettes. A typical experiment included 15−20 samples (2−3 μM protein for visible measurements and 5−8 μM protein for CD measurements) with varying concentrations of urea in a total volume of 400 μL. For denaturation experiments, the protein solutions for each sample in a data set were made up using gastight syringes and allowed to equilibrate at 25 °C for at least 16 h before the absorbance at 409 nm, or the CD signal at 222 nm, was recorded. Curves that describe a two-state unfolding transition were fit to independent sets of denaturation data (obtained from CD experiments) by the method of Santoro and Bolen (*46*). The values of $\Delta G°_{H_2O}$ and m_g reported in Table 2 are averages of three or four independent denaturation experiments. The values of C_m reported in Table 2 were obtained by taking the first derivative of the fitted curves.

Refolding curves were obtained by dilution of the fully unfolded protein into buffer with a lower denaturant con-

Table 1: Ligand Binding Kinetic Data for Wild-Type and Permuted Myoglobins[a]

parameter	HGL16	swMb
CO_{on} ($\times 10^{-6}$ M^{-1} s^{-1})	0.63	0.50 (0.50)
CO_{off} (s^{-1})	0.017	.021 (0.018)
K_{CO} ($\times 10^{-6}$ M^{-1})	37	24 (28)
O_{2on} ($\times 10^{-6}$ M^{-1} s^{-1})	18	16 (16)
O_{2off} (s^{-1})	15	18 (17)
K_{O_2} ($\times 10^{-6}$ M^{-1})	1.2	0.89 (0.9)

[a] Protein samples in 100 mM phosphate buffer (pH 7.0) at 20 °C. Numbers in parentheses are the kinetic constants for wild-type myoglobin reported in ref *35*.

Table 2: Stability Parameters for Wild-Type and Permuted Myoglobins at 25 °C and pH 7.5

parameter	HGL16	swMb
$\Delta G°_{H_2O}$ (kcal/mol)	7.2 ± 0.5	12.4 ± 1.6
m_g (kcal mol^{-1} M^{-1})	-1.65 ± 0.11	-1.83 ± 0.23
C_m (M urea)	4.19 ± 0.05	6.90 ± 0.06

centration. Oxidized protein was prepared as described above and added to concentrated urea to a final denaturant concentration of approximately 9 M urea. These solutions were allowed to equilibrate at 25 °C for 16−24 h. The unfolded protein in denaturant was then diluted into buffer to a final volume of 400 μL and a final protein concentration of approximately 5 μM. The diluted samples were allowed to equilibrate for 16−24 h, and absorbance at 409 nm, or CD at 222 nm, was measured as described above.

Nuclear Magnetic Resonance Studies. Protein samples for NMR studies were converted to the paramagnetic cyanomet isoform by addition of 1.2 heme equivalents of potassium ferricyanide and 1.7 heme equivalents of potassium cyanide. The cyanomet proteins were then injected onto an HPSEC column (Amersham Pharmacia Biotech Superdex 75 HR 10/30) attached to an HPLC system (Varian ProStar) and equilibrated with 20 mM potassium phosphate (pH 7.5). The buffer-exchanged proteins were concentrated (Amicon Centricon YM-10 concentrators) until the total volume was approximately 400−500 μL, and D_2O was added. The final concentrations of the NMR samples were estimated, by optical measurement at 423 nm, to be 0.29 mM (with 30% D_2O) for the wild-type swMb and 0.30 mM for the HGL16 permutein (with 10% D_2O). The wild-type swMb sample appeared to have a larger amount of the reversed heme-insertion isomer (*47*) than the HGL16 sample (this phenomenon will be addressed in a later study); thus, it has an apparent lower concentration than the HGL16 permutein.

NMR spectra were acquired on a Bruker AMX-400 spectrometer, using a dedicated 5 mm proton probe. SUPERWEFT data were collected as described previously (*48*), employing short delays to saturate the longer relaxing resonances. To assign the proton chemical shifts, phase-sensitive NOESY (*49*) with TPPI (*50*) and magnitude-COSY (*51*) spectra were recorded, and then compared to previous assigned resonances for the cyanomet form of native swMb (*52*). Data were processed using either SwaN-MR (*53*, *54*) or nmrPipe (*55*). Two-dimensional spectra were zero-filled in both dimensions to give 2048 × 2048 real matrices, and polynomial baseline corrections were applied as needed. Two-dimensional spectra were analyzed and plotted using nmrView (*56*).

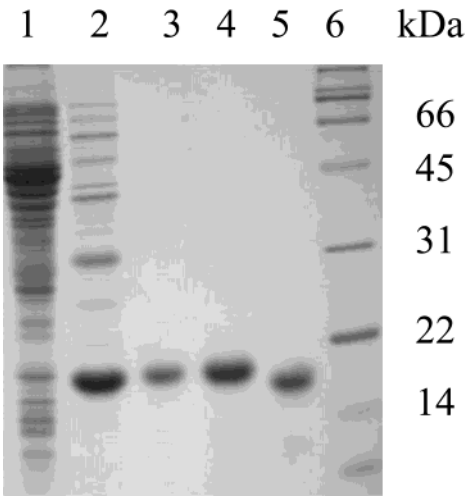

FIGURE 2: HGL16 is purified to >95% homogeneity by a two-column procedure. A Coomassie-stained 15% SDS−PAGE gel is shown: lane 1, induced HGL16 cell culture; lane 2, IMAC-purified HGL16; lane 3, 2 μg of HPSEC-purified HGL16; lane 4, 10 μg of HPSEC-purified HGL16; lane 5, HPSEC-purified recombinant swMb; and lane 6, protein molecular mass markers.

RESULTS

Expression. Wild-type and permuted myoglobins were expressed in either DH5α, XL1-blue, or BL21(DE3) *E. coli* cells. Yields of the purified permutein range from 0.6 to 1.2 mg/L of shake flask culture. Western blot analysis (not shown) showed that the HGL16 protein was optimally expressed 4 h postinduction in all three strains.

Purification. The recombinant myoglobins were purified using an efficient two-column protocol to >95% homogeneity as judged by SDS−PAGE (Figure 2). The electrophoretic mobility of HGL16 is slightly retarded compared to that of wild-type swMb due to the addition of the 16-amino acid linker. HGL16 and wild-type swMb coelute by HPSEC over a concentration range of 5−500 μM (not shown), indicating that the folded permutein is monomeric. Amino acid sequencing and mass spectrometry of purified HGL16 (and its tryptic fragments) confirmed the expected mass of the permutein as well as the location of the H helix and the linker (Figure 1). In addition, we found that the N-terminal Met residue had been removed. The post-translational cleavage of an N-terminal Met that is followed by Ala or Gly is known for the expression of globins in *E. coli* (*57*, *58*).

Ligand Binding. Association and dissociation rates for the binding of carbon monoxide or oxygen to HGL16 display single-exponential decay (Figure 3), and are not significantly different from those for the wild-type protein (Table 1). The permutein HGL16 appears to have a slightly higher affinity for these ligands than wild-type swMb. The similarity in functional properties suggests that the structures of the two proteins are also similar.

Structure. The far-UV CD spectrum of HGL16 shows strong α-helical character, and the near-UV CD spectra of HGL16 and wild-type myoglobin show similar shape and fine structure (not shown). Further evidence that the permutein appears to fold with nativelike structure is provided by one- and two-dimensional NMR analyses.

^{1}H NMR spectroscopy of a paramagnetic heme protein's hyperfine-shifted resonances is an exquisitely sensitive probe of structural changes in the vicinity of the heme. For

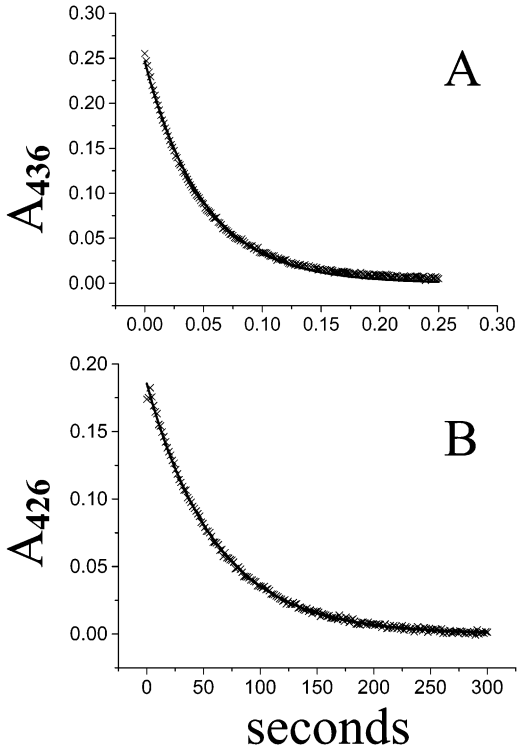

FIGURE 3: Stopped-flow ligand binding data show the single-exponential decay. (A) CO binding to HGL16. (B) CO dissociation from HGL16. Data points are shown with the symbol ×, and a solid line shows the best fit curves for single-exponential decay. Kinetic constants and comparisons to the wild-type protein are given in Table 1.

myoglobins and hemoglobins, the cyanomet form offers a very high degree of resolution, resulting from relatively narrow line widths and a reasonable dispersion of chemical shifts (*59*). Figure 4 shows one-dimensional (1D) NMR spectra for both wild-type swMb and HGL16, both as "normal" acquisitions and as SUPERWEFT (*48*) experiments, which provide reduced relative intensities for peaks that have longer relaxation times, showing that they are farther from the paramagnetic center. These spectra demonstrate a remarkable degree of chemical shift similarity between the cyanomet forms of HGL16 and wild-type swMb in the vicinity of the heme pocket, with nearly identical heme chemical shifts, and only mildly perturbed chemical shifts for the indicated amino acids that are close enough to the heme iron to be shifted into these regions. Other compelling evidence for the similarity of the heme pocket structures is found in the patterns of NOEs from the hyperfine shift-resolved resonances, shown by the comparisons in Figures 5 and 6 for the downfield and upfield peak NOE patterns, respectively. These spectra provide direct evidence for such similarity between the proteins because they present both chemical shifts and proton−proton distance relationships.

The most immediately obvious difference between the NMR data of the two proteins is the ∼0.85 ppm downfield shift in Ile FG5 CγH on going from wild-type swMb to HGL16 (Figure 4). Also, there are ∼0.96 and ∼0.28 ppm upfield shifts in His F8 CϵH and Phe CD1 CζH, respectively. Other notable highly shifted resonances from the heme pocket residues, His E7 NϵH and His F8 NδH, show very little chemical shift change (∼0 and ∼0.09 ppm upfield, respectively) on going from wild-type swMb to HGL16 (Figure 4). Most heme resonances have almost no differences in chemical shifts, with the exception that 1-CH_3 shifts ∼0.26 ppm upfield, while the 2-Hα experiences an ∼0.08 ppm downfield shift (both of these are from the same heme pyrrole). Interestingly, this last resonance is the sole hyperfine-shifted resonance to exhibit a significant shift away from its diamagnetic position on going from wild-type swMb to HGL16.

Stability. The urea denaturation isotherms of wild-type swMb obtained by monitoring heme absorbance (a measure of myoglobin tertiary structure) or CD (a measure of secondary structure) are superimposable (Figure 7A), indicating that the unfolding of the protein is cooperative and very likely two-state. The overlap of the corresponding isotherms obtained with HGL16 is good in the pretransition region and through the first half of the unfolding transition. In the latter portion of the unfolding transition, the isotherms diverge. We believe this divergence is an artifact that is the result of nonspecific binding of heme to denatured permutein, as has been described by Hargrove and Olson (*30*) during the chemical denaturation of destabilized myoglobin mutants. Nonspecific heme binding would give rise to increased values for heme absorbance as the concentration of denatured permutein increases during the unfolding transition (at concentrations of urea that are insufficiently high to disrupt the nonspecific binding of the heme to the denatured permutein). The unfolding of HGL16 in urea therefore appears to be cooperative and two-state (Figure 7). Superimposable isotherms are obtained for the unfolding of native HGL16 permutein, and for the refolding of denatured permutein, demonstrating that the unfolding of HGL16 is reversible under the conditions of the denaturation experiments. Curves describing a theoretical two-state unfolding transition fit very well to the denaturation data (Figure 7C). The stability parameters obtained by curve fitting are shown in Table 2. The unfolding transition for HGL16 is highly cooperative with a value of m_g that is not significantly different from that of the wild-type protein; however, relative to wild-type swMb, HGL16 appears to be destabilized by 5.2 kcal/mol.

DISCUSSION

The major conclusion drawn from published reports describing the circular permutation of several proteins is that the folded, functional tertiary structure of a protein is not necessarily determined by the *order* of secondary structural elements in the protein (*18*, *41*, *42*, *60*−*62*) [however, this may be a general property observed only for proteins with a stability of greater than roughly 7 kcal/mol (*63*)]. Likewise, our data show that the order of the helices in the primary sequence of sperm whale myoglobin can be changed and a stable, functional protein can be recovered.

The isolated yields of purified HGL16 permutein from shake flask cultures (0.6−1.2 mg/L) are substantially lower than the yields of purified wild-type swMb obtained under similar fermentation conditions. Hargrove et al. (*25*) have reported that expression yields of myoglobin point mutants are correlated to the stability of the mutant against chemical denaturation; thus, the reduced expression yields of HGL16 relative to wild-type swMb suggest that HGL16 is a less stable myoglobin variant. Western blot analysis of protein

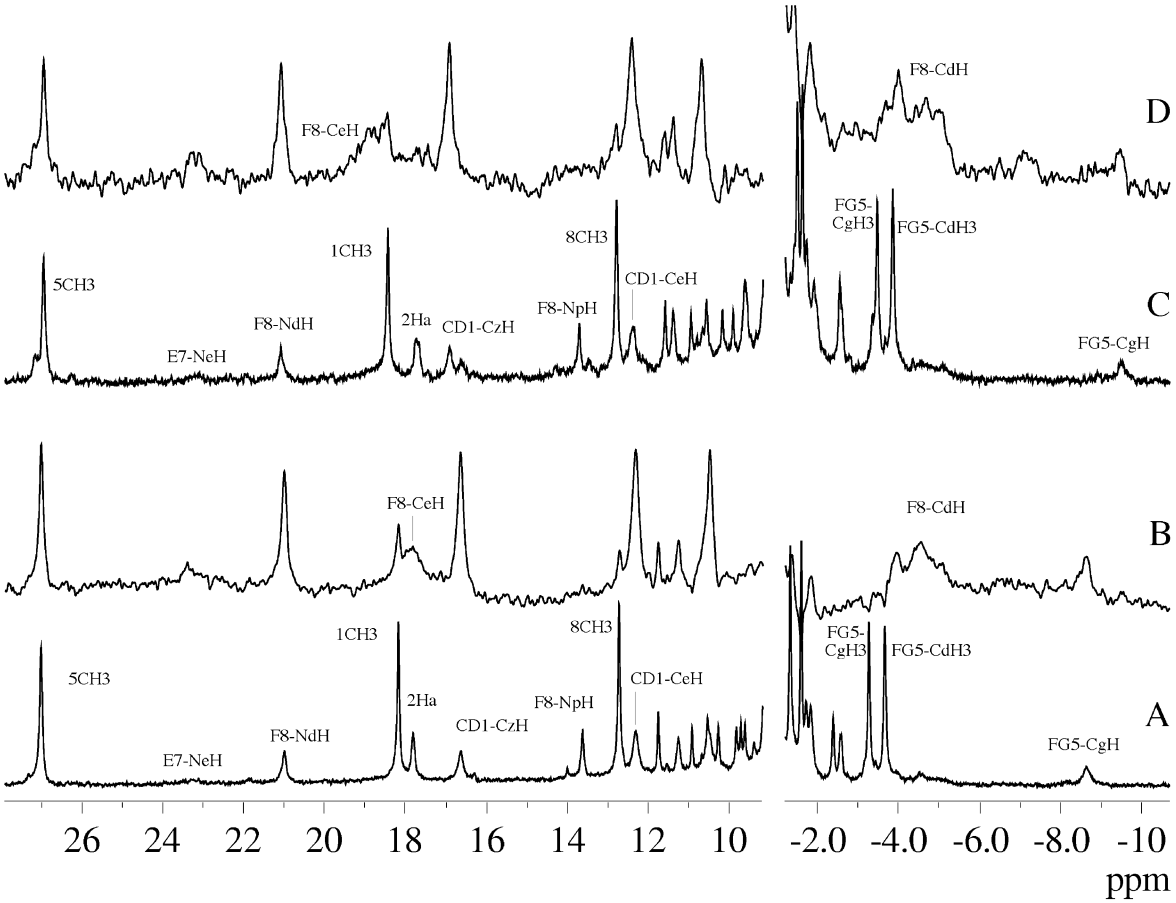

FIGURE 4: One-dimensional ^{1}H NMR hyperfine shift-resolved regions of spectra of HGL16 and wild-type swMb. (A) Standard spectrum of HGL16. (B) SUPERWEFT spectrum of HGL16. (C) Standard spectrum of wild-type swMb. (D) SUPERWEFT spectrum of wild-type swMb. A few key resonance assignments are provided. Note that the SUPERWEFT spectra provide for reduced intensities for the slower-relaxing resonances, which are those that are farthest from the paramagnetic iron center. The "standard spectra" were acquired at 30 °C in ^1H_2O at pH 7.5 (see Experimental Procedures), with a 90° observation pulse and an ~1.5 s low-power solvent saturation pulse, giving a total recycle time of ~1.6 s for each of the 128 scans. The SUPERWEFT spectra were acquired with an 80 ms low-power solvent presaturation pulse and a 50 ms delay between the 180° pulse and the 90° observation pulse, giving a total recycle time of ~140 ms for each of the 128 scans.

expression as a function of time (data not shown) provides more direct evidence for the decreased stability of the HGL16 permutein relative to wild-type swMb. The permutein shows the greatest accumulation 4−5 h postinduction. The concentration of permutein decreases after 6 h until it is not detectable 19 h postinduction. This is in sharp contrast to the wild-type protein, which shows increasing accumulation through 19 h postinduction.

The effects of permutation on ligand binding are slight (Table 1), and the permutein appears to adopt a well-defined, nativelike folded structure (Figure 4). The data in Table 1 show that CO and O_2 binding to the HGL16 permutant are minimally perturbed compared to wild-type swMb, and that HGL16 binds both ligands with slightly increased affinity. This observation is also supported by autoxidation data. Ferrous oxy-HGL16 autoxidizes more slowly than does wild-type myoglobin (A. V. Lissounov and S. J. Anthony-Cahill, unpublished observation). The rate of autoxidation in myoglobin has been shown to be inversely proportional to the equilibrium dissociation constant for ligand binding (*64*). The modest changes in ligand binding behavior suggest that the heme pocket adopts a conformation that is very close to the wild-type conformation.

The ^{1}H NMR data presented in Figures 4−6 give direct evidence that the heme pocket does, in fact, adopt a conformation that is very close to that found in wild-type swMb. The nearly identical heme chemical shifts indicate that the unpaired spin density must be highly similar for these two proteins. This likewise is evidence that the proximal His F8 ring is at approximately the same angle, relative to the heme N−Fe−N axes, for the two proteins. The similarity of NOE intensities between the 5-CH_3 and each of the two 6H_α resonances indicates that at least this propionate is in approximately the same orientation; thus, the salt bridge to Arg CD3 is most likely intact. The differences in chemical shifts for the 3-CH_3 and 2H_α *might* arise from a slightly perturbed angle of the 2-vinyl, relative to the heme plane; however, the similarity between the 2H_α NOE patterns for the two proteins dictates that such a difference would be slight. Further experiments would be needed to establish such a subtle structural and/or dynamical difference. The differences in heme pocket residue chemical shifts are most notable for residues FG5 (proximal) and CD1 (distal). These chemical shift differences may point toward a small change in the Fe−CN ligand tilt between HGL-16 and wild-type swMb (*65*), although a much more detailed analysis, based upon a large set of assigned amino acid resonances, would be required to establish this with a high degree of certainty. Likewise, it is possible that these changes could arise from other small perturbations in the structure of the heme pocket.

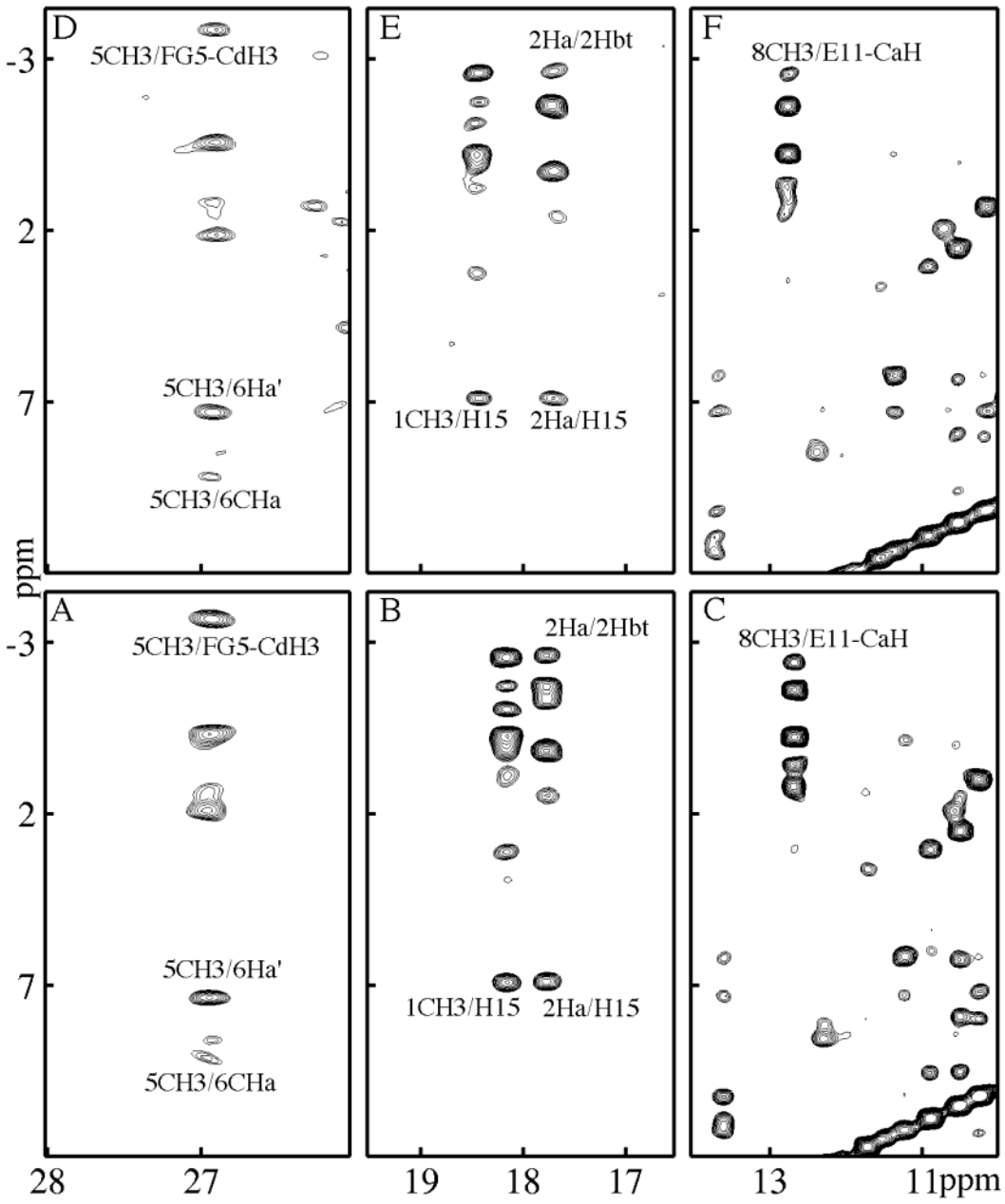

FIGURE 5: Downfield regions of 2D NOESY spectra of HGL16 and wild-type swMb: HGL16 (A−C) and wild-type swMb (D−F). A few key cross-peak identities are provided. Note the overall correspondence of panels A and D, B and E, and C and F, showing that the NOE (distance-dependent) contacts are virtually identical in these two proteins. The spectra were recorded at 30 °C in ^1H_2O at pH 7.5 (see Experimental Procedures), with a 100 ms mixing time, a 1.5 s low-power solvent saturation pulse, and 128 scans per free induction decay, as two identical 1024 × 512 data sets that were summed after processing.

Also as seen in Figure 4, the region between 9 and 12 ppm has several resonances that are in nearly the same place. Many of these are labile, and so must arise from amino acid residues. This is further evidence for a largely conserved heme pocket structure. In summary, the NMR data show that the heme pocket structures in these two proteins are not identical, but they are certainly very similar.

Whereas the ligand binding function and structure of the permutein closely resemble those of wild-type swMb, the stabilities of the permuted and wild-type myoglobins are significantly different. With few exceptions, circular permuteins show stabilities that are reduced compared to those of the parent proteins. Reported values of $\Delta\Delta G°_{H_2O}$ for unfolding [i.e., $\Delta G°_{H_2O}$(wild type) − $\Delta G°_{H_2O}$(permutein)] range from 1 kcal/mol for T4 lysozyme (*61*) and 1.4−1.8 kcal/mol for the α-spectrin SH3 domain (*41*) to 5−7 kcal/mol for RNase T1 (*42*). The $\Delta\Delta G°_{H_2O}$ of 5.2 kcal/mol (Table 2) we observe for HGL16 is within the range of values reported for other circular permuteins. It should be noted that the 21 Å distance between the N- and C-termini observed in the X-ray crystal structure (*66*) of swMb is one of the largest distances spanned by a linker in a circular permutein. We chose a very long linker to span this distance to ensure minimal perturbation of any structure that might be required for proper folding of the permutein at the ends of the A and H helices.

It is tempting to speculate that a long flexible linker composed of serine and glycine residues would destabilize the permutein relative to wild-type swMb due to entropic stabilization of the unfolded state relative to the folded state

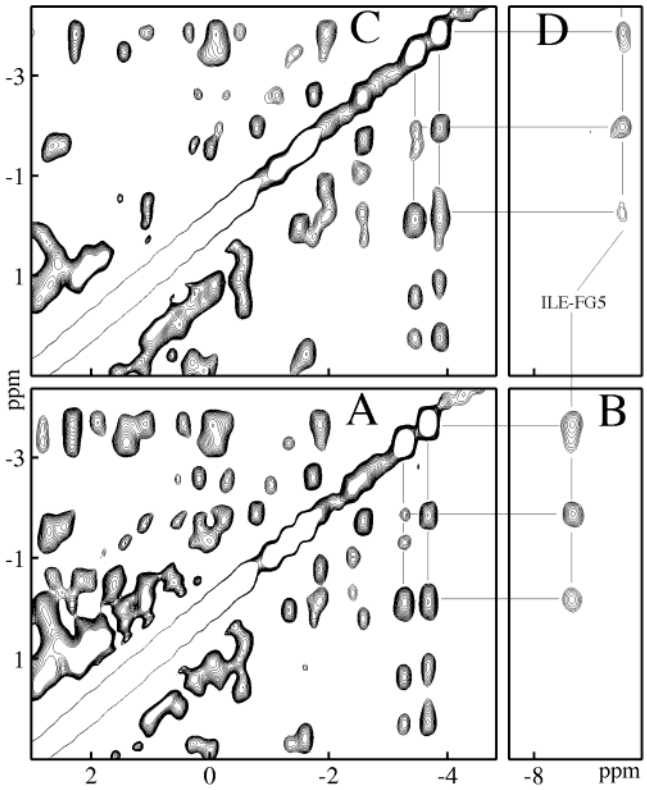

FIGURE 6: Upfield regions of 2D NOESY spectra of HGL16 (A and B) and wild-type swMb (C and D). A few key cross-peaks, for residue Ile FG5, are indicated. Note the overall correspondence of panels A and C, and B and D, showing that the NOE (distance-dependent) contacts in this region are very similar in these two proteins. The spectra were acquired as indicated in the legend of Figure 5.

(*1*). For circular permutants of dihydrofolate reductase, it has been shown that the length of the flexible peptide linking the original termini can significantly affect the stability of the permutein (*67*). To assess the effects of linker length on the stability of the HGL16 permutein, we have purified permuteins that have 9−12 flexible amino acids (i.e., Gly and Ser) in the linker. On the basis of preliminary unfolding data, there are no significant differences in $\Delta G^{\circ}_{H_2O}$ between any of these permuteins (J. R. Keeffe and S. J. Anthony-Cahill, unpublished observation). If we consider the linker in the permutein to be analogous to a loop, this observation is consistent with a report that the destabilizing effect associated with flexible loops is linearly correlated with increasing loop length between two and ten residues, and then plateaus (*68*). We have also isolated a permutein that has five amino acids in the linker. This permutein appears to bind heme; however, it is significantly destabilized compared to the other permuteins we have generated (V. J. Terrill and S. J. Anthony-Cahill, unpublished observation), suggesting that the optimum linker length may be between five and nine residues.

The work described herein shows that sperm whale myoglobin can tolerate topological mutation. This is a significant finding for two reasons. First, a thorough understanding of the topological constraints of the globin fold could lead to the design of recombinant human hemoglobins with altered topology, or a single-chain hemoglobin, with improved therapeutic properties (*69*−*72*). In fact, the successful permutation of a single-chain dialpha globin (which can bind two beta globins to form a functional hemoglobin molecule) has been described (*37*). Second, the apo forms of circularly permuted myoglobins will be useful in future studies of the effects of topology on folding kinetics (the apo form of HGL16 appears to fold stably at 25 °C; A. V. Lissounov and S. J. Anthony-Cahill, unpublished observation).

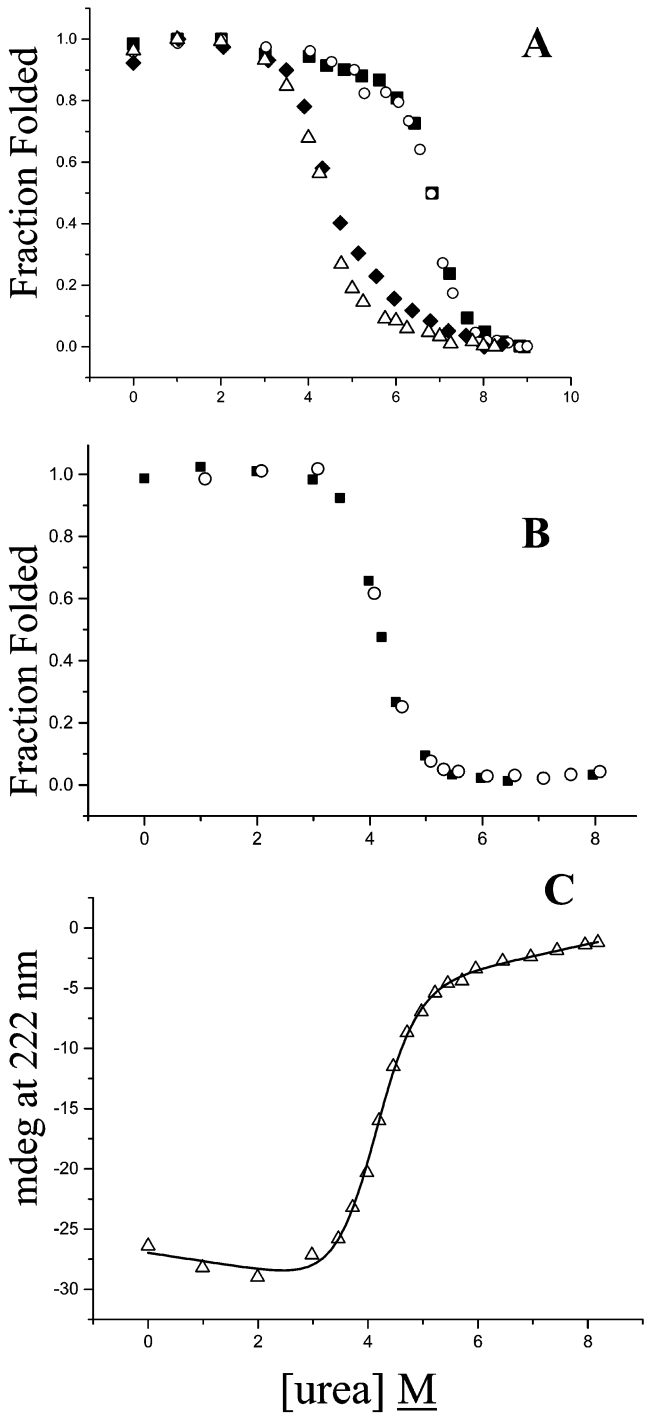

FIGURE 7: Chemical denaturation isotherms of wild-type swMb and HGL16 permutein. (A) Normalized CD signal at 222 nm for swMb (○) and HGL16 (△) and normalized heme absorbance at 409 nm for swMb (■) and HGL16 (◆). The divergence of the isotherms for HGL16 is an artifact of nonspecific heme binding (see the text). (B) Normalized CD signal at 222 nm for the unfolding (■) and refolding (○) of HGL16. (C) CD signal at 222 nm for the unfolding of HGL16 (△, same data set as that shown in panel A) showing the fit of a theoretical two-state unfolding curve (—).

An interesting feature of apomyoglobin folding is the formation of an early intermediate composed of amino acids primarily in the A, G, and H helices (*13*). This folding intermediate bears strong structural similarity to the acid-stabilized "molten globule" state of apomyoglobin (*23*). The fast phase of apomyoglobin folding, in which the denatured protein collapses to the early folding intermediate, is associated with the formation of helical structure in parts of the A, G, and H helices. We will be particularly interested in the characterization of the folding kinetics of circularly permuted apomyoglobins in which the positions of these three helices are shifted relative to the protein termini. The HGL16 permutein shifts the H helix to the N-terminus, but the A, G, and H helices are still positioned at the protein termini in a manner that is comparable to the arrangement of these helices in the wild-type protein (i.e., in HGL16, the H and A helices are N-terminal and the G helix is C-terminal, whereas in wild-type swMb, the A helix is N-terminal and the G and H helices are C-terminal). If the folding of apo-HGL16 also involves rapid collapse of the A, G, and H helices, the entropic cost (or benefit) of that collapse may be similar to that of wild-type apomyoglobin since the majority of the protein sequence is constrained between these terminal helices in both cases (*73*). In contrast, a permutein that positions these three helices in the center of the protein sequence would not constrain the apoprotein termini during a rapid hydrophobic collapse involving the A, G, and H helices. To improve our understanding of protein design and structure prediction, it would be informative to identify the early folding elements in a protein and determine how the placement of these elements within the protein primary sequence affects folding rates, or more generally, the folding pathway. Permuteins of myoglobin, including the one described herein, should allow us to address these fundamental questions in protein folding, stability, and design in a well-characterized system.

ACKNOWLEDGMENT

We express thanks to Professor John Olson for providing the swMb gene, access to stopped-flow instrumentation in his laboratory, and sharing his expertise in myoglobin structure−function studies, Dr. Antony Mathews for expert instruction in the use of stopped-flow instrumentation, Sam Schaefer-Joel for providing cloning intermediates used in the construction of the swMb tandem gene template, Dr. Ray Paxton and Dr. Rich Johnson for protein analytical data, Dr. Richard Remmele and Duke Phan for the initial CD characterization of HGL16, and Professor Lisa Gentile for a critical reading of the manuscript.

REFERENCES

1. Matthews, B. W., Nicholson, H., and Becktel, W. J. (1987) Enhanced protein thermostability from site-directed mutations that decrease the entropy of unfolding, *Proc. Natl. Acad. Sci. U.S.A. 84*, 6663−6667.
2. Shortle, D. (1989) Probing determinants of protein folding and stability with amino acid substitutions, *J. Biol. Chem. 264*, 5315−5318.
3. Perry, L. J., and Wetzel, R. (1984) Disulfide bond engineered into T4 lysozyme: stabilization of the protein toward thermal inactivation, *Science 226*, 555−557.
4. Sauer, R. T., Hehir, K., Stearman, R. S., Weiss, M. A., Jeitler-Nilsson, A., Suchanek, E. G., and Pabo, C. O. (1986) An engineered intersubunit disulfide enhances the stability and DNA binding of the N-terminal domain of λ repressor, *Biochemistry 25*, 5992−5998.
5. Matsumura, M., Signor, G., and Matthews, B. W. (1989) Substantial increase of protein stability by multiple disulphide bonds, *Nature 342*, 291−293.
6. Mitchinson, C., and Wells, J. A. (1989) Protein engineering of disulfide bonds in subtilisin BPN′, *Biochemistry 28*, 4807−4815.
7. Zhao, H., Giver, L., Shao, Z., Affholter, J. A., and Arnold, F. H. (1998) Molecular evolution by staggered extension process (StEP) in vitro recombination, *Nat. Biotechnol. 16*, 258−261.
8. Shoichet, B. K., Baase, W. A., Kuroki, R., and Matthews, B. W. (1995) A relationship between protein stability and protein function, *Proc. Natl. Acad. Sci. U.S.A. 92*, 452−456.
9. Puri, R. K., Hoon, D. S., Leland, P., Snoy, P., Rand, R. W., Pastan, I., and Kreitman, R. J. (1996) Preclinical development of a recombinant toxin containing circularly permuted interleukin 4 and truncated *Pseudomonas* exotoxin for therapy of malignant astrocytoma, *Cancer Res. 56*, 5631−5637.
10. Brinkmann, U., Di Carlo, A., Vasmatzis, G., Kurochkina, N., Beers, R., Lee, B., and Pastan, I. (1997) Stabilization of a recombinant F_v fragment by base-loop interconnection and V_H-V_L permutation, *J. Mol. Biol. 268*, 107−117.
11. McWherter, C. A., Feng, Y., Zurfluh, L. L., Klein, B. K., Baganoff, M. P., Polazzi, J. O., Hood, W. F., Paik, K., Abegg, A. L., Grabbe, E. S., Shieh, J.-J., Donnelly, A. M., and McKearn, J. P. (1999) Circular permutation of the granulocyte colony-stimulating factor receptor agonist domain of myelopoietin, *Biochemistry 38*, 4564−4571.
12. Englander, S. W., and Mayne, L. (1992) Protein folding studied using hydrogen-exchange labelling and proton NMR, *Annu. Rev. Biophys. Biomol. Struct. 21*, 243−265.
13. Jennings, P. A., and Wright, P. E. (1993) Formation of a molten globule intermediate early in the kinetic folding pathway of apomyoglobin, *Science 262*, 892−896.
14. Fersht, A. (1994) Characterizing transition states in protein folding: an essential step in the puzzle, *Curr. Opin. Struct. Biol. 5*, 79−84.
15. Viguera, A. R., Serrano, L., and Wilmanns, M. (1996) Different folding transition states may result in the same native structure, *Nat. Struct. Biol. 3*, 874−880.
16. Otzen, D. E., and Fersht, A. R. (1998) Folding of circular permuted chymotrypsin inhibitor 2: Retention of the folding nucleus, *Biochemistry 37*, 8139−8146.
17. Hennecke, J., Sebbel, P., and Glockshuber, R. (1999) Random circular permutation of DsbA reveals segments that are essential for protein folding and stability, *J. Mol. Biol. 286*, 1197−1215.
18. Iwakura, M., Nakamura, T., Yamane, C., and Maki, K. (2000) Systematic circular permutation of an entire protein reveals essential folding elements, *Nat. Struct. Biol. 7*, 580−585.
19. Graf, R., and Schachman, H. K. (1996) Random circular permutation of genes and expressed polypeptide chains: Application of the method to the catalytic chains of aspartate transcarbamoylase, *Proc. Natl. Acad. Sci. U.S.A. 93*, 11591−11596.
20. Baird, G. S., Zacharias, D. A., and Tsien, R. Y. (1999) Circular permutation and receptor insertion within green fluorescent proteins, *Proc. Natl. Acad. Sci. U.S.A. 96*, 11241−11246.
21. Springer, B. A., and Sligar, S. G. (1987) High level expression of sperm whale myoglobin in *Escherichia coli*, *Proc. Natl. Acad. Sci. U.S.A. 84*, 8961−8965.
22. Hughson, F. M., and Baldwin, R. L. (1989) Use of site-directed mutagenesis to destabilize native apomyoglobin relative to folding intermediates, *Biochemistry 28*, 4415−4422.
23. Hughson, F. M., Wright, P. E., and Baldwin, R. L. (1990) Structural characterization of a partly folded apomyoglobin intermediate, *Science 249*, 1544−1548.
24. Lin, L., Pinker, R. J., Forde, K., Rose, G. D., and Kallenbach, N. R. (1994) Molten globular characteristics of the native state of apomyoglobin, *Nat. Struct. Biol. 1*, 447−452.
25. Hargrove, M. S., Kryzwda, S., Wilkinson, A. J., Dou, Y., Ikeda-Saito, M., and Olson, J. S. (1994) Stability of myoglobin: a model for the folding of heme proteins, *Biochemistry 33*, 11767−11775.
26. Griko, Y. V., and Privalov, P. L. (1994) Thermodynamic puzzle of apomyoglobin unfolding, *J. Mol. Biol. 235*, 1318−1325.
27. Kiefhaber, T., and Baldwin, R. L. (1995) Intrinsic stability of individual alpha helices modulates structure and stability of the apomyoglobin molten globule form, *J. Mol. Biol. 252*, 122−132.
28. Loh, S., Kay, M., and Baldwin, R. (1995) Structure and stability of a second molten globule intermediate in the apomyoglobin folding pathway, *Proc. Natl. Acad. Sci. U.S.A. 92*, 5446−5450.

29. Kay, M. S., and Baldwin, R. L. (1996) Packing interactions in the apomyoglobin folding intermediate, *Nat. Struct. Biol. 3*, 439−445.
30. Hargrove, M. S., and Olson, J. S. (1996) The stability of holomyoglobin is determined by heme affinity, *Biochemistry 35*, 11310−11318.
31. Ballew, R. M., Sabelko, J., and Gruebele, M. (1996) Direct observation of fast protein folding: the initial collapse of apomyoglobin, *Proc. Natl. Acad. Sci. U.S.A. 93*, 5759−5764.
32. Jamin, M., and Baldwin, R. L. (1996) Refolding and unfolding kinetics of the equilibrium folding intermediate of apomyoglobin, *Nat. Struct. Biol. 3*, 613−618.
33. Cavagnero, S., Dyson, H. J., and Wright, P. E. (1999) Effect of H helix destabilizing mutations on the kinetic and equilibrium unfolding of apomyoglobin, *J. Mol. Biol. 285*, 269−282.
34. Mathews, A. J., Rohlfs, R. J., Olson, J. S., Tame, J., Renaud, J.-P., and Nagai, K. (1989) The effects of E7 and E11 mutations on the kinetics of ligand binding to R state human hemoglobin, *J. Biol. Chem. 264*, 16573−16583.
35. Rohlfs, R. J., Mathews, A. J., Carver, T. E., Olson, J. S., Springer, B. A., Egeberg, K. D., and Sligar, S. G. (1990) The effects of amino acid substitution at position E7 (residue 64) on the kinetics of ligand binding to sperm whale myoglobin, *J. Biol. Chem. 265*, 3168−3176.
36. Doherty, D. H., Doyle, M. P., Curry, S. R., Vali, R. J., Fattor, T. J., Olson, J. S., and Lemon, D. D. (1998) Rate of reaction with nitric oxide determines the hypertensive effect of cell-free hemoglobin, *Nat. Biotechnol. 16*, 672−676.
37. Sanders, K. E., Lo, J., and Sligar, S. G. (2002) Intersubunit permutation of human hemoglobin, *Blood 100*, 299−305.
38. Barrick, D., and Baldwin, R. L. (1993) Three-state analysis of sperm whale apomyoglobin folding, *Biochemistry 32*, 3790−3796.
39. Eliezer, D., Yao, J., Dyson, H. J., and Wright, P. E. (1998) Structural and dynamic characterization of partially folded states of apomyoglobin and implications for protein folding, *Nat. Struct. Biol. 5*, 148−155.
40. Feng, Z., Ha, J.-H., and Loh, S. N. (1999) Identifying the site of initial tertiary structure disruption during apomyoglobin unfolding, *Biochemistry 38*, 14433−14439.
41. Viguera, A. R., Blanco, F. J., and Serrano, L. (1995) The order of secondary structure elements does not determine the structure of a protein but does affect its folding kinetics, *J. Mol. Biol. 247*, 670−681.
42. Johnson, J. L., and Rauschel, F. M. (1996) Influence of primary sequence transpositions on the folding pathways of ribonuclease T1, *Biochemistry 35*, 10223−10233.
43. Pappu, R. V., and Weaver, D. L. (1998) The early folding kinetics of apomyoglobin, *Protein Sci. 7*, 480−490.
44. Antonini, E., and Brunori, M. (1971) *Hemoglobin and Myoglobin in Their Reactions with Ligands*, Elsevier, North-Holland, New York.
45. Pace, C. N. (1986) Determination and analysis of urea and guanidine hydrochloride denaturation curves, *Methods Enzymol. 131*, 266−280.
46. Santoro, M. M., and Bolen, D. W. (1988) Unfolding free energy changes determined by the linear extrapolation method. 1. Unfolding of phenylmethylsulfonyl α-chymotrypsin using different denaturants, *Biochemistry 27*, 8063−8068.
47. Jue, T., Krishnamoorthi, R., and La Mar, G. N. (1983) Proton NMR study of the mechanism of the heme-apoprotein reaction for myoglobin, *J. Am. Chem. Soc. 105*, 5701−5703.
48. Inubishi, T., and Becker, E. D. J. (1983) Efficient detection of paramagnetically shifted NMR resonances by optimizing the WEFT sequence, *J. Magn. Reson. 51*, 128−133.
49. Kumar, A., Ernst, R. R., and Wüthrich, K. (1980) A two-dimensional nuclear Overhauser enhancement (2D NOE) experiment for the elucidation of complete proton−proton cross-relaxation networks in biological macromolecules, *Biochem. Biophys. Res. Commun. 95*, 1−6.
50. Marion, D., and Wüthrich, K. (1983) Application of phase sensitive two-dimensional correlated spectroscopy (COSY) for measurements of $^1H-^1H$ spin−spin coupling constants in proteins, *Biochem. Biophys. Res. Commun. 113*, 967−974.
51. La Mar, G. N., and de Ropp, J. S. (1993) NMR Methodology for Paramagnetic Proteins, in *Biological Magnetic Resonance* (Berliner, L. J., and Rebuen, J., Eds.) pp 1−78, Plenum Press, New York.
52. Emerson, S. D., and La Mar, G. N. (1990) Solution structural characteristics of cyanometmyoglobin: resonance assignment of heme cavity residues by two-dimensional NMR, *Biochemistry 29*, 1545−1556.
53. Balacco, G. (1994) SwaN-MR: A complete and expansible NMR software for the Macintosh, *J. Chem. Inf. Comput. Sci. 34*, 1235−1241.
54. Balacco, G. (2000) SwaN-MR: from infancy to maturity, *Mol. Biol. Today 1*, 23−28.
55. Delaglio, F., Grzesiek, S., Vuister, G. W., Zhu, G., Pfeifer, J., and Bax, A. (1995) NMRPipe: a multidimensional spectral processing system based on UNIX pipes, *J. Biomol. NMR 6*, 277−293.
56. Johnson, B. A., and Blevins, R. A. (1994) NMRView: A computer program for the visualization of NMR data, *J. Biomol. NMR 4*, 603−614.
57. Hirel, P. H., Schmitter, J. M., Dessen, P., Fayat, G., and Blanquet, S. (1989) Extent of N-terminal methionine excision from *Escherichia coli* proteins is governed by the side-chain length of the penultimate amino acid, *Proc. Natl. Acad. Sci. U.S.A. 86*, 8247−8251.
58. Apostol, I., Aitken, J., Levine, J., Lippincott, J., Davidson, J. S., and Abbott-Brown, D. (1995) Recombinant protein sequences can trigger methylation of N-terminal amino acids in *Escherichia coli*, *Protein Sci. 4*, 2616−2618.
59. La Mar, G. N., Satterlee, J. D., and de Ropp, J. S. (1999) Nuclear Magnetic Resonance of Hemoproteins, in *The Porphyrin Handbook* (Kadish, K. M., Smith, K. M., and Guilard, R., Eds.) pp 185−298, Academic Press, San Diego.
60. Horlick, R. A., George, H. J., Cooke, G. M., Tritch, R. J., Newton, R. C., Dwivedi, A., Lischwe, M., Salemme, F. R., Weber, P. C., and Horuk, R. (1992) Permuteins of interleukin 1 beta: a simplified approach for the construction of permutated proteins having new termini, *Protein Eng. 5*, 427−431.
61. Zhang, T., Bertelsen, E., Benvegnu, D., and Alber, T. (1993) Circular permutation of T4 lysozyme, *Biochemistry 32*, 12311−12318.
62. Yang, Y. R., and Schachman, H. K. (1993) Aspartate transcarbamoylase containing circularly permuted catalytic polypeptide chains, *Proc. Natl. Acad. Sci. U.S.A. 90*, 11980−11984.
63. Smith, V. F., and Matthews, C. R. (2001) Testing the role of chain connectivity on the stability and structure of dihydrofolate reductase from *E. coli*: Fragment complementation and circular permutation reveal stable, alternatively folded forms, *Protein Sci. 10*, 116−128.
64. Brantley, R. E., Smerdon, S. J., Wilkinson, A. J., Singleton, E. W., and Olson, J. S. (1993) The mechanism of autooxidation of myoglobin, *J. Biol. Chem. 268*, 6995−7010.
65. Emerson, S. D., and La Mar, G. N. (1990) NMR determination of the orientation of the magnetic susceptibility tensor in cyanometmyoglobin: a new probe of steric tilt of bound ligand, *Biochemistry 29*, 1556−1566.
66. Watson, H. C. (1969) The Stereochemistry of the Protein Myoglobin, *Prog. Stereochem. 4*, 299.
67. Iwakura, M., and Nakamura, T. (1998) Effects of the length of a glycine linker connecting the N- and C-termini of a circularly permuted dihydrofolate reductase, *Protein Eng. 11*, 707−713.
68. Viguera, A.-R., and Serrano, L. (1997) Loop length, intramolecular diffusion and protein folding, *Nat. Struct. Biol. 4*, 939−946.
69. Winslow, R. M. (1992) *Hemoglobin-based Red Cell Substitutes*, Johns Hopkins University Press, Baltimore.
70. Looker, D., Abbott-Brown, D., Cozart, P., Durfee, S., Hoffman, S., Mathews, A. J., Miller-Roehrich, J., Shoemaker, S., Trimble, S., Fermi, G., Komiyama, N. H., Nagai, K., and Stetler, G. L. (1992) A human recombinant haemoglobin designed for use as a blood substitute, *Nature 356*, 258−260.
71. Gould, S. A., Sehgal, L. R., Sehgal, H. L., and Moss, G. S. (1995)-The development of hemoglobin solutions as red cell substitutes: Hemoglobin solutions, *Transfus. Sci. 16*, 5−17.
72. D'Agnillo, F., and Chang, T. M. S. (1998) Polyhemoglobin-superoxide dismutase-catalase as a blood substitute with antioxidant properties, *Nat. Biotechnol. 16*, 667−671.
73. Zhang, T., Bertelsen, E., and Alber, T. (1994) Entropic effects of disulphide bonds on protein stability, *Nat. Struct. Biol. 1*, 434−438.

BI026404G